ACS Sustainable Chemistry & Engineering

pubs.acs.org/journal/ascecg

Research Article

Regiodivergent Isosorbide Acylation by Oxidative N-Heterocyclic Carbene Catalysis in Batch and Continuous Flow

Daniele Ragno,* Costanza Leonardi, Graziano Di Carmine, Olga Bortolini, Arianna Brandolese, Carmela De Risi, and Alessandro Massi*

Cite This: *ACS Sustainable Chem. Eng.* 2021, 9, 8295−8305

Read Online

ACCESS | Metrics & More | Article Recommendations | Supporting Information

ABSTRACT: A new N-heterocyclic carbene (NHC)-catalyzed strategy for the regioselective monoesterification of isosorbide (IS) at either the endo (5-OH) or exo (2-OH) position is described. Site-selective acylation proceeds under oxidative conditions in the presence of a quinone oxidant using aldehydes as mild acylating agents. Experimental evidences suggest a role of the stereoelectronic features of the acyl azolium salt intermediate in determining the selectivity of the acylation process. The solvent effect was also investigated, considering conventional and sustainable solvents. Aromatic aldehydes, including bio-based furfural and 5-hydroxymethyl furfural, together with α,β-unsaturated aldehydes proved to be effective reaction partners affording monoacyl-isosorbides with satisfactory levels of regioselectivity (exo/endo: 5.3−3.5; endo/exo: 5.3−3.3). Additionally, the exo-selective triazolium salt promoter was successfully transferred into the heterogeneous phase and applied to continuous-flow catalysis. In particular, the polystyrene-supported version of the selected NHC showed a catalytic activity comparable to that of the homogeneous counterpart in terms of both conversion efficiency (turnover number = 108) and regioselectivity (exo/endo up to 5.3). Also, the corresponding packed-bed mesoreactor was operated with long-term stability (ca. 110 h on stream) to produce 2-benzoyl-IS (1.32 mmol h^{-1} $mmol_{cat}^{-1}$), which is the key intermediate in the synthesis of a commercial active pharmaceutical ingredient, namely, the vasodilator isosorbide-5-mononitrate.

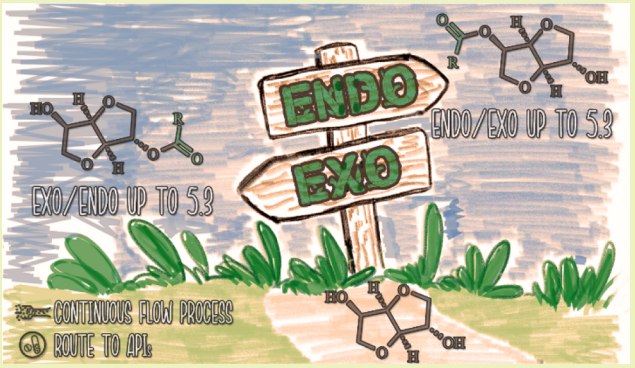

KEYWORDS: *renewable, platform chemicals, packed-bed reactor, organocatalysis, heterogeneous catalyst, flow chemistry, esters*

INTRODUCTION

In recent years, biomass waste utilization has become a main focus of research activities in industry and academia for the production of bio-based platform chemicals by fractionalization or manipulation of lignocellulosic sources.[1] Among these, a compound of growing importance is isosorbide (IS; 1,4:3,6-dianhydro-D-glucitol), which is a renewable diol produced on an industrial scale by the hydrogenation of glucose to sorbitol, followed by double dehydration.[2,3] IS is a chiral, rigid, nontoxic molecule displaying two secondary hydroxyl groups in endo and exo configurations and a V-shaped backbone composed of fused furan units (Figure 1).[4,5] The two nonequivalent hydroxyl groups of IS show different reactivities: the *endo*-5-OH is more nucleophilic than the *exo*-2-OH due to the intramolecular hydrogen bonding with the oxygen of the adjacent furan ring, but it is also more sterically hindered because of its position within the folded bicyclic structure. Until now, IS has been efficiently converted into different high value-added products for applications in the pharmaceutical,[6,7] surfactant,[8−10] plasticizer,[11,12] polymer,[13−20] and catalysis[21,22] fields. The regioselective functionalization of the 2- and 5-hydroxyl groups is often the key for a successful strategy toward valuable IS-based products, the endo and exo derivatives being typically endowed with different chemical, biological, and physical properties. Indeed, the commercial vasodilator isosorbide-5-mononitrate (**IS-5MN**) is preferred in the clinic over isosorbide-2-mononitrate and isosorbide-dinitrate because of its advantageous pharmacokinetics (Figure 1).[23] Also, in the polymer field, different physical behaviors of polymethacrylates prepared from regioisomeric IS-based vinyl monomers have been reported (Figure 1).[24,25] Hence, the definition of efficient regioselective protocols for the monofunctionalization of IS is of great interest in the biorefinery context. In particular, the selective acylation leading to the monoesters of IS is an attractive process, which is currently used in a number of multistep syntheses based on protection/

Received: April 24, 2021
Revised: May 26, 2021
Published: June 8, 2021

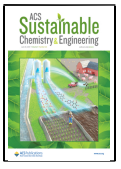

https://doi.org/10.1021/acssuschemeng.1c02765
ACS Sustainable Chem. Eng. 2021, 9, 8295−8305

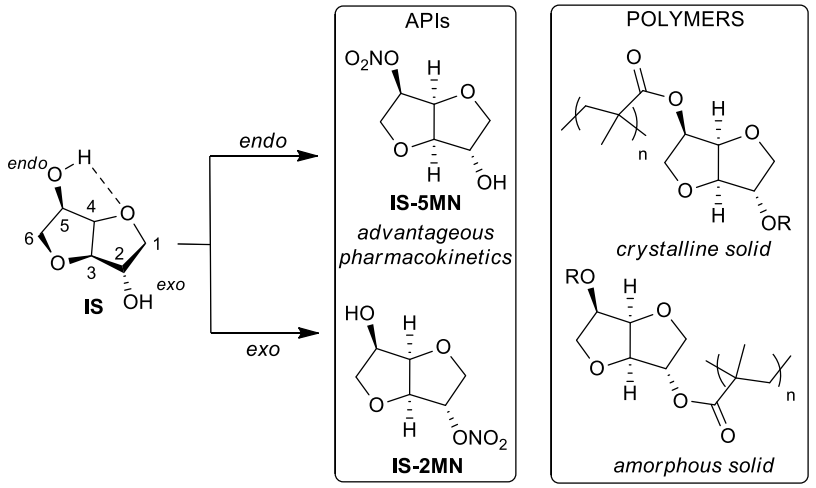

Figure 1. Regioselective acylation of IS, leading to active pharmaceutical ingredients (APIs) and polymers.

Scheme 1. NHC-Catalyzed Synthesis of *endo*- and *exo*-MAIs

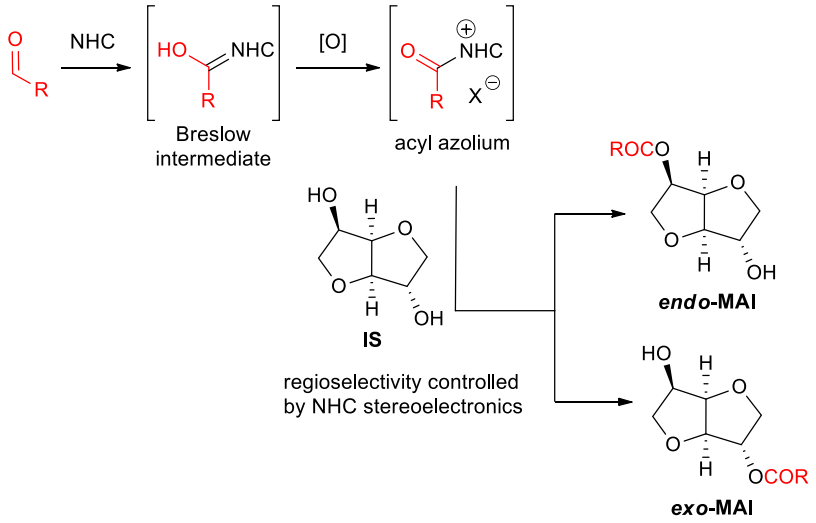

deprotection strategies. Acylation is typically favored at the endo position in virtue of the more nucleophilic character of 5-OH; effective reported metal catalysts for endo acylation are the harmful PbO[26−28] and, more suitably, $Sc(OTf)_3$ for greener and selective processes (*endo*-acetate/*exo*-acetate = 4.2:1).[29] Selectivity at the exo position is, instead, achieved by *N*,*N*′-dicyclohexylcarbodiimide (DCC)-mediated couplings of the less hindered 2-OH with carboxylic acids in the presence of 4-dimethylaminopyridine (DMAP); this process proceeds with low atom economy and moderate selectivity, exploiting the steric bulkiness of the *O*-acyl isourea intermediate.[30,31] Additionally, more specialized biocatalytic approaches have been developed with high levels of either endo- or exo-selectivity.[24,32−35]

To the best of our knowledge, the only fully regiodivergent synthesis of 2- and 5-isosorbide monoesters (acetyl derivatives) has been described by Aldabbagh and co-workers, who utilized equimolar or excess MeMgCl to attain selective acetylation at the endo or exo position, respectively, through controlled alkoxide magnesium salt formation.[36] Downside of this effective methodology is, however, the need of stoichiometric amounts of the basic organometallic reagent. Quite surprisingly, organocatalytic strategies for IS monoesterification have not been reported in the literature so far. In continuation of our studies on the upgradation of bio-based feedstocks by oxidative N-heterocyclic carbene (NHC) catalysis,[37−44] we present herein the regiodivergent synthesis of *endo*- and *exo*-monoacylisosorbides (MAIs) by the use of aldehydes as mild acylating agents (Scheme 1), including the biorefinery products furfural (FF) and 5-hydroxymethyl furfural (HMF). Although not fully rationalized yet, the origin of the observed regioselectivity seems to lie primarily in the different stereoelectronic properties of the catalytically generated acyl azolium (oxidation of the Breslow intermediate), which may undergo attack by either *endo*-5-OH or *exo*-2-OH (Scheme 1). Significantly, the developed methodology proved to be effective with the heterogeneous version of the selected NHC promoter (polystyrene support) and compatible with a continuous-flow (CF) setup by the fabrication of the corresponding packed-bed mesoreactors.

RESULTS AND DISCUSSION

The regioselective benzoylation of IS **2** with benzaldehyde **1a** was selected as the benchmark using the quinone **5** as the stoichiometric oxidant and a suitable base (25 mol %) for the precatalyst **A**−**E** activation (Table 1). Thiazolium salt **A** (10 mol %) in combination with NEt_3 [anhydrous tetrahydrofuran

https://doi.org/10.1021/acssuschemeng.1c02765
ACS Sustainable Chem. Eng. 2021, 9, 8295−8305

Table 1. Optimization Study with Precatalysts A–E in Conventional Solvents[a]

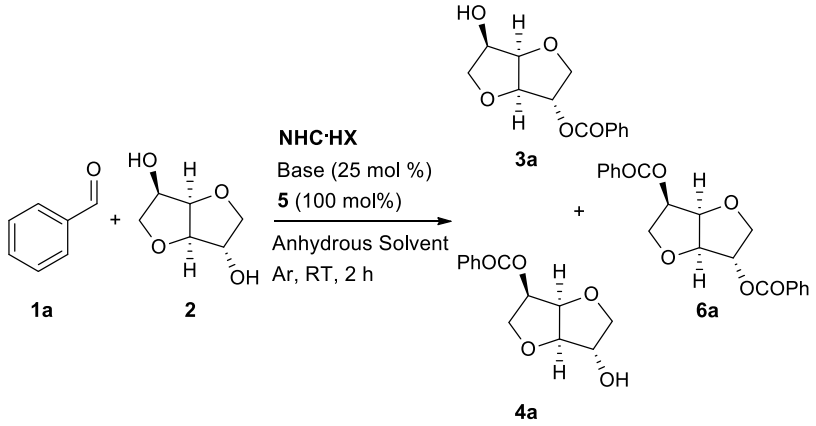

entry	NHC·HX (mol %)	base	solvent	**3a** (%)[b]	**4a** (%)[b]	**6a** (%)[b]
1[c]	**A** (10)	NEt_3	THF	36	24	10
2[c]	**B** (10)	DBU	THF			
3	**C** (10)	DBU	THF	40	24	33
4[d]	**C** (10)	DBU	THF	69	23	6
5[d]	**C (5)**	**DBU**	**THF**	**76**	**17**	**5**
6[d]	**C** (5)	DBU	DCM	75	18	5
7[c,d]	**C** (5)	DBU	toluene	45	44	5
8[c,d]	**C** (5)	DBU	DMSO	30	27	
9[d]	**C** (5)	DBU	DMF	45	43	10
10[d]	**D** (5)	NEt_3	THF	22	50	22
11[d]	**D** (5)	NEt_3	DCM	49	38	7
12[d]	**D** (5)	NEt_3	toluene			60
13[d]	**D (5)**	**NEt_3**	**DMSO**	**15**	**78**	**5**
14[c,d,e]	**D** (5)	NEt_3	DMSO	29	35	
15[d]	**E** (5)	DBU	THF	30	60	5

[a]**1a** (0.50 mmol), **2** (0.50 mmol), and anhydrous solvent (4.0 mL). [b]Detected by ^{1}H NMR of the crude reaction mixture with durene as the internal standard. [c]Reaction time: 24 h. [d]**2** (1.50 mmol). [e]$CaCl_2$ (0.56 mmol).

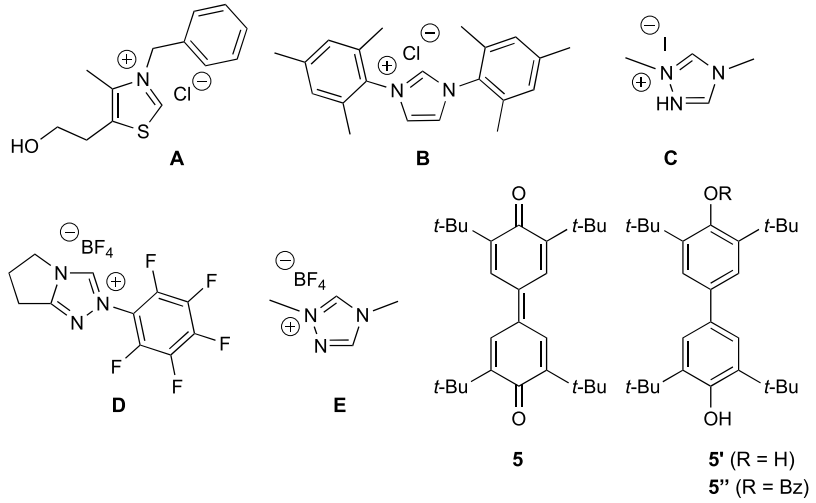

(THF), room temperature, 24 h] led to the partial conversion of equimolar **1a**/**2** with little selectivity (*exo*-MAI **3a**, 36%; *endo*-MAI **4a**, 24%; diester **6a**, 10%. Entry 1). Under the same conditions, the imidazolium salt **B**/1,8-diazabicyclo[5.4.0]-undec-7-ene (DBU) couple was completely inactive (entry 2). The system made of triazolium salt **C** (10 mol %) and DBU provided high conversion after 2 h, accompanied, however, by low regioselectivity and formation of a considerable amount of diester **6a** (33%, entry 3). Afterward, the reaction conditions were tuned with **C** in order to limit the competitive–consecutive diester formation and, eventually, increase the regioselectivity of the process. Indeed, the use of excess IS (3 equiv), which is easily recoverable by aqueous work-up thanks to its water solubility, corresponded to a decrease of **6a** yield (6%) and a promising level of exo-regioselectivity (**3a**/**4a** = 69:23; entry 4). Satisfyingly, this result could be improved by reducing the catalyst loading to 5 mol % (**3a**/**4a** = 76:17; entry 5). The replacement of THF with dichloromethane (DCM) resulted in an almost identical reaction outcome (entry 6), while the utilization of toluene afforded a lower regioselectivity and

https://doi.org/10.1021/acssuschemeng.1c02765
ACS Sustainable Chem. Eng. 2021, 9, 8295–8305

required longer reaction times (entry 7). Polar aprotic solvents dimethyl sulfoxide (DMSO) and dimethylformamide (DMF) produced poorer results (entries 8 and 9), with the formation of a considerable amount of benzoic acid byproduct (30% yield) in DMSO. The exo-selectivity observed under the optimal conditions of entries 5 and 6 (exo/endo = 4.5) was tentatively rationalized in terms of steric hindrance of the acyl azolium salt generated from **C**[45] and the consequent preferential attack by the more accessible *exo*-2-OH, in analogy with the DCC-mediated esterification of IS based on the generation of *O*-acyl isourea intermediates.[30,31]

In a previous investigation on regioselective acylative desymmetrization of glycerol, we detected a peculiar and different reactivity of the *N*-pentafluorophenyl pyrrolidine-based triazolium salt **D** compared to **C**.[38] Therefore, the precatalyst **D** was screened in the model IS benzoylation using THF as the solvent, and a modest but significant switch in regioselectivity (**3a**/**4a** = 22:50) was observed (entry 10). Surprisingly, the use of DCM in place of THF restored the preferential, though modest, exo-selectivity (**3a**/**4a** = 49:38, entry 11), thus suggesting an important role of the solvent in directing regioselectivity with **D**. The use of toluene provided diester **6a** (60%) as the main product together with the monobenzoylated hydroquinone **5″** (38%), which was unexpectedly formed by acylation of the highly hindered diol **5′** (entry 12). Gratifyingly, the solvent change to polar aprotic DMSO resulted in a satisfactory level of endo-selectivity (endo/exo = 5.2) and reduced diester formation (**3a**/**4a** = 15:78, **6a** = 5%, entry 13). Although a complete rationalization of the origin of regioselectivity is premature at this stage of our study, it can be envisaged that an intermolecular hydrogen bonding between the more nucleophilic 5-OH and the acyl azolium salt generated from **D** might play a central role in promoting the endo-selectivity of entry 13, in analogy with an earlier study reporting IS acylations in the presence of metal chlorides.[46] Additional experimental evidences consist in the loss of regioselectivity when using $CaCl_2$ as an additive in combination with **D** (entry 14)[46] and the switch back to preferential endo-selectivity with triazolium salt **E** that displays the same azolium structure of the exo-selective **C** and BF_4^- in place of I^- as the counterion (entry 15 vs entry 5). These latter results further confirm the importance of counterions in directing NHC catalysis[47] and, in this specific study, strengthen our hypothesis that the endo-selectivity of the disclosed IS esterification is mainly controlled by electronic factors, which are responsible for 5-OH nucleophilicity enhancement by intermolecular hydrogen-bonding interactions.[46] This appears evident with the precatalyst **D**, which is highly endo-selective in DMSO having a strong hydrogen-bond-accepting (HBA) character (entry 13) and moderately exo-selective in noncoordinating DCM (entry 11). In the case of the precatalyst **C**, the effect on regioselectivity of the solvent HBA ability is also observed as this promoter is highly exo-selective in DCM (entry 6) and almost unselective in DMSO (entry 8). Overall, it can be hypothesized that the NHC-catalyzed benzoylation of IS preferentially occurs at the less sterically hindered *exo*-2-OH in solvents with poor HBA character because of the intrinsic bulkiness of the acyl azolium intermediates generated from both **C** and **D**;[45] on the contrary, esterification proceeds at the more nucleophilic *endo*-5-OH if intermolecular hydrogen-bonding interactions are activated by the presence of a suitable coordinating solvent and/or counterion (Scheme 2).[48,49] Actually, the real nature of the acyl azolium counterion is difficult to predict as other ionic

Scheme 2. Tentative Rationalization of the Origin of Regioselectivity in NHC-Catalyzed IS Esterification (HBA: Hydrogen-Bonding-Accepting)

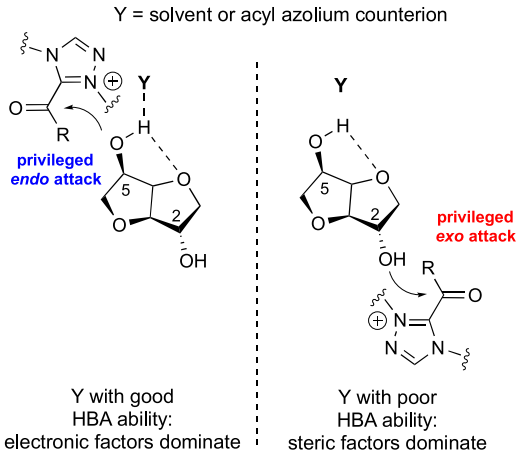

species are present in the reaction mixture, including the phenolate generated from **5′** and the ammonium salt produced from the nitrogen base during free NHC formation. All these variables further complicate the mechanistic picture that is currently the object of a dedicated computational study aimed at gaining more insights and understanding.

The catalytic activity of triazolium salts **C** and **D** was also tested in selected green solvents to improve the sustainability of the disclosed regiodivergent IS acylation (Table 2).[50−55] Bio-based polar aprotic solvents were initially screened with the **C**/DBU couple. Utilization of 2-methyltetrahydrofuran (Me-THF) resulted in long reaction times and moderate exo-selectivity (**3a**/**4a** = 59:25, entry 1), while γ-valerolactone (GVL) and dimethyl isosorbide (DMI) completely inhibited the model acylation process (entries 2 and 3). As expected, ethyl lactate (EL) consumed the in situ-generated acyl azolium, producing benzoyl EL as the sole isolable product (entry 4). Acetylcholine chloride−urea was selected as the convenient deep eutectic solvent (DES),[56] but poor results in terms of conversion and regioselectivity were detected in this reaction medium (entry 5).

Table 2. Optimization Study with Precatalysts C and D in Sustainable Solvents[a]

entry	NHC·HX (mol %)	base	solvent	**3a** (%)[b]	**4a** (%)[b]	**6a** (%)[b]
1[c]	**C** (5)	DBU	Me-THF	59	25	7
2[c]	**C** (5)	DBU	GVL			
3[c]	**C** (5)	DBU	DMI			
4[c]	**C** (5)	DBU	EL			
5[c]	**C** (5)	DBU	DES[d]	17	15	
6[c]	**C** (5)	DBU	LIM	10	9	
7	**D** (5)	NEt_3	Me-THF	45	50	5
8	**D** (5)	NEt_3	GVL	47	49	
9	**D** (5)	NEt_3	DMI	37	54	6
10	**D** (5)	NEt_3	EL			
11	**D** (5)	NEt_3	DES[d]	40	45	
12	**D** (5)	NEt_3	LIM			56

[a]For the structures of reagents, precatalysts, products, and by-products, see Table 1. **1a** (0.50 mmol), **2** (1.50 mmol), solvent (4.0 mL), 4 Å molecular sieves, reaction time: 3 h. [b]Detected by ^{1}H NMR of the crude reaction mixture, with durene as the internal standard. [c]Reaction time: 24 h. [d]DES: acetylcholine chloride−urea.

https://doi.org/10.1021/acssuschemeng.1c02765
ACS Sustainable Chem. Eng. 2021, 9, 8295−8305

Next, (*R*)-(+)-limonene (LIM) was tested as the representative apolar bio-based solvent, detecting the prevalent formation of benzil (80%; entry 6); this byproduct (not shown) was generated by in situ oxidation of benzoin, which in turn was preferentially formed by homocoupling of benzaldehyde **1a** as a consequence of the low solubility of IS in limonene. At this stage, the same selection of sustainable solvents was screened using the precatalyst **D** in combination with NEt_3. In general, application of this catalytic system determined faster kinetics compared to **C**/DBU, affording full conversion of **1a** in about 3 h. In particular, the model benzoylation proceeded in Me-THF and GVL with no selectivity (entries 7 and 8), while the use of DMI preferentially gave *endo*-MAI **4a** (**3a**/**4a** = 37:54, entry 9). Again, EL competed with IS in the acylation process, producing benzoyl EL (entry 10). Disappointingly, the utilization of acetylcholine chloride−urea resulted in the formation of an almost equimolar mixture of **3a** and **4a** (entry 11). Finally, limonene produced similar results to those obtained in toluene (Table 1, entry 12), affording the diester **6a** (56%) and the benzoylated hydroquinone **5″** (40%; entry 12). On the whole, this explorative study with the selection of green solvents revealed the superior performance of THF/DCM and DMSO in directing the exo- and endo-regioselectivity, respectively, of IS esterification, thus justifying the application of these conventional solvents in the proposed methodology. This choice is in accordance with the solvent selection guides (SSGs) contributed from pharmaceutical industries,[53,57,58] which cover the different aspects of greenness in addition to the environmental impact, including solvent stability, recyclability, handling, storage, toxicity, and life cycle impact. Based on the above SSGs, it is observed that DCM, THF, and DMSO display acceptable environmental health and safety characteristics, which allow for their use in the synthesis of APIs and speciality chemicals.[59]

The regioselective acylation of IS was next examined with the representative classes of aldehydes **1** to prepare a set of *exo*-MAIs **3** (Table 3) and *endo*-MAIs **4** (Table 4). Although THF and DCM gave comparable results in the benchmark with the **C**/DBU catalytic system, the former solvent was preferred in the synthesis of *exo*-MAIs **3** because of its better environmental acceptability. Aromatic o- and p-substituted chlorobenzaldehydes **1b,c** afforded the corresponding *exo*-MAIs **3b,c** with good efficiency (entries 2 and 3). A complete conversion of **1b,c** was observed in 1 h without the detection of byproducts derived from the competitive benzoin reaction,[39] thus confirming the higher reactivity of electron-poor aromatic aldehydes in the acylation of secondary alcohols by oxidative NHC catalysis. Actually, anisaldehyde **1d** and *p*-tolualdehyde **1e** were consumed more slowly, showing, however, satisfactory levels of regioselectivity (entries 4 and 5). Next, the sugar-derived FF **1f** and HMF **1g** were tested with the aim to synthesize fully bio-based conjugates of IS.[60,61] FF **1f** was highly reactive and gave MAI **3f** with the highest detected value of exo-selectivity (exo/endo = 5.3, entry 6). The effective combination of IS with HMF **1g** required a large excess of IS **2** (20 equiv) to minimize the production of oligoesters derived from HMF homocoupling, as observed in our previous studies;[38,40] under these conditions, unreacted IS was efficiently recovered by aqueous work-up, and the *exo*-HMF−IS conjugate **3g** was produced in satisfactory 65% isolated yield. Of note, diol **3g** is a novel, renewable monomer that is currently under investigation in our laboratories for the production of bio-based polyesters with unexplored potential in the polymer field.[38] Finally, cinnamaldehyde **1h** was considered as the representative substrate of α,β-unsaturated aldehydes, affording *exo*-MAIs **3h** with good efficiency (76% yield; exo/endo = 4.6; entry 8). Unfortunately, all the attempts to extend the disclosed methodology to saturated aliphatic aldehydes failed because of the competitive aldol reaction that preferen-

Table 3. Regioselective Synthesis of *exo*-MAIs 3a−h[a]

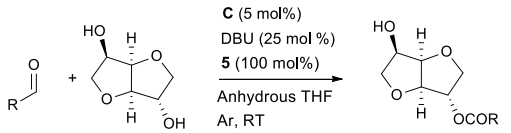

Entry	Aldehyde	3 (%)[b]	exo:endo[c]
1	1a	3a (72)	4.6
2	1b	3b (70)	4.3
3	1c	3c (71)	4.0
4	1d	3d (68)	3.5
5	1e	3e (74)	4.3
6	1f	3f (74)	5.3
7[d]	1g	3g (65)	4.0
8	1h	3h (76)	4.6

[a]**1a−h** (0.5 mmol), **2** (1.5 mmol), and anhydrous THF (4.0 mL). Isolated yields of *endo*-MAIs **4** and diesters **6** are reported in the Supporting Information. [b]Isolated yield. [c]Selectivity detected by ^{1}H NMR of the crude reaction mixture. [d]**2** (20 equiv, 10.0 mmol).

https://doi.org/10.1021/acssuschemeng.1c02765
ACS Sustainable Chem. Eng. 2021, 9, 8295−8305

Table 4. Regioselective Synthesis of *endo*-MAIs 4a−h[a]

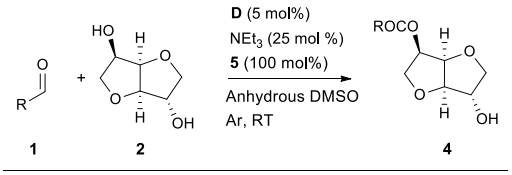

Entry	Aldehyde	4 (%)[b]	endo:exo[c]
1	 1a	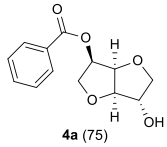 4a (75)	5.3
2	 1b	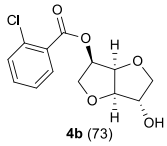 4b (73)	4.9
3	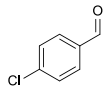 1c	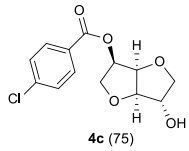 4c (75)	4.6
4	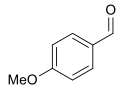 1d	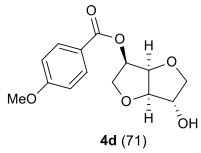 4d (71)	3.8
5	 1e	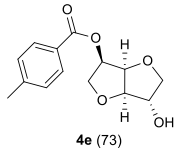 4e (73)	4.3
6	 1f	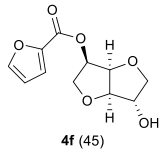 4f (45)	3.3
7[d]	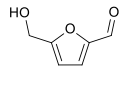 1g	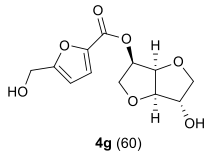 4g (60)	4.0
8	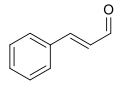 1h	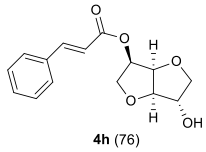 4h (76)	4.6

[a]**1a−h** (0.5 mmol), **2** (1.5 mmol), and anhydrous DMSO (4.0 mL). Isolated yields of *exo*-MAIs **3** and diesters **6** are reported in the Supporting Information. [b]Isolated yield. [c]Selectivity detected by ^{1}H NMR of the crude reaction mixture. [d]**2** (20 equiv, 10.0 mmol).

tially occurred in the basic reaction medium. Nevertheless, it is important to point out that the disclosed oxidative acylation strategy represents, together with enzyme-mediated approaches,[34,35] the only direct catalytic method to access IS monoesters with exo-selectivity, showing the advantage of a good tolerance to variation in the aldehyde acylating agents.

The same aldehyde−IS combinations were also investigated under the optimized conditions of entry 13 (Table 1) to access *endo*-MAIs **4a−h** (Table 4). The registered values of reaction yield (45−76%) and regioselectivity (endo/exo = 5.3−3.8) were comparable to those of the model reaction, with the exception of FF **1f**−IS coupling (entry 6), where selectivity (endo/exo = 3.3) was partially eroded by the unavoidable side reaction leading to diester **6f** (40%).

Driven by our experience in process intensification by NHC immobilization and transition to the CF regime,[39,40,62−64] we initially explored the setup of an effective batch procedure for the model benzoylation of IS at the exo position, which is the key step in the synthesis of valuable IS derivatives.[23,65] Hence, the utilization of the polystyrene-supported version of triazolium salt **C** was considered. Typically, NHC immobilization allows for easy catalyst separation/recycling and may limit carbene deactivation induced by air and moisture, thus improving the productivity and sustainability of the whole synthetic protocol.[62−64] In order to verify the effect of catalyst site isolation on reaction efficiency,[66,67] heterogeneous triazolium salts **F−G** were readily prepared from the Merrifield resin with different degrees of functionalization (**F**, *f*: 0.93 mmol g^{-1}; **G**, *f*: 0.47 mmol g^{-1}; Table 5).[39] First, immobilized triazolium salt **F** (5 mol %) was tested under the optimized conditions of the homogeneous process (THF, room temperature), but a longer reaction time (16 h) and almost no regioselectivity were observed (entry 1). Satisfyingly, the solvent change to anhydrous DCM improved the swelling properties of the polystyrene support and led to the full conversion of **1a** in 2 h with improved exo-selectivity (exo/endo = 2.8, entry 2). To our delight, a significant increase of regioselectivity was registered, with **G** displaying a lower degree of functionalization (exo/endo

Table 5. Optimization Study with Heterogeneous Precatalysts F and G[a]

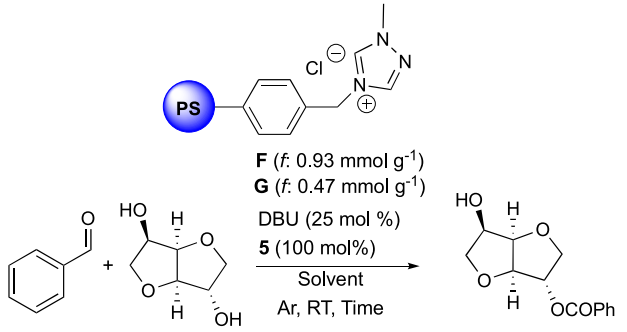

entry	NHC·HX (mol %)	solvent	time (h)	yield (%)[b]	exo/endo[c]
1	**F** (5)	THF	16	57	1.4
2	**F** (5)	DCM	2	72	2.8
3	**G (5)**	**DCM**	**3**	**80**	**4.4**
4	**G** (2)	DCM	16	71	3.7
5	**G** (5)	Me-THF	24	61	2.1
6	**G** (5)	DES[d]	48	7	1.1
7[e]	**G** (5)	DCM	3	68	4.5

[a]**1a** (0.50 mmol), **2** (1.50 mmol), and anhydrous solvent (4.0 mL). [b]Detected by ^{1}H NMR of the crude reaction mixture, with durene as an internal standard. [c]Selectivity detected by ^{1}H NMR of the crude reaction mixture. [d]DES: acetylcholine chloride−urea. [e]Fifth recycle.

https://doi.org/10.1021/acssuschemeng.1c02765
ACS Sustainable Chem. Eng. 2021, 9, 8295−8305

= 4.4, entry 3). According to our mechanistic hypothesis, this result can be explained by a reduced effect of intermolecular hydrogen bonding on *endo*-5-OH nucleophilic enhancement, which could be favored by the presence on the surface of adjacent azolium units. Unfortunately, the reduction of catalyst loading (from 5 to 2 mol %) determined a marked decrease of reaction efficiency (entry 4). As expected, on the basis of the study with the soluble triazolium salt **C** (Table 2), utilization of Me-THF and acetylcholine chloride−urea resulted in only a partial conversion of **1a,** even at longer reaction times and in very low exo-selectivities (entries 5 and 6). Finally, the recyclability of the precatalyst **G** was investigated over six runs, with DCM as the preferred solvent (Figure 2). Catalyst recovery consisted in

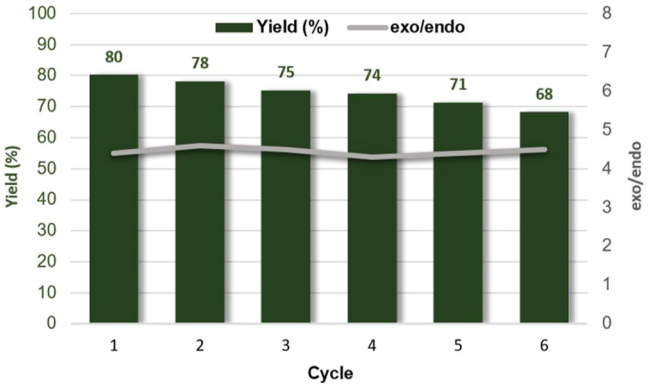

Figure 2. Recycling experiments (**1a**/**2** coupling promoted by **G**).

the simple filtration, washing, and drying of the resin. Gratifyingly, only a moderate decrease (~3%) of conversion efficiency with unaltered regioselectivity was detected after each recycle, achieving an accumulated turnover number (TON) of 108 (entry 7). The sustainability of the heterogeneous oxidative monoesterification could be further improved by the easy recovery of DCM (distillation) and of the stoichiometric oxidant. Actually, the diol **5′**, which is quantitatively produced from quinone **5** during the acylation process (Table 1), was readily separated and reoxidized to **5** with air in the presence of catalytic phthalocyanine, as detailed in the Supporting Information for a gram-scale experiment.

The robustness of the heterogeneous procedure with the active triazolium precatalyst **G** (5 mol %) was confirmed by reproducing the aldehyde−IS combinations of the homogeneous process with comparable levels of efficiency (Table 6).

Quite interestingly, the coupling product of IS and HMF **1g** promoted by **G** gave the bis-adduct **3g′** (74%) displaying two HMF units (Scheme 3). Reasonably, despite the use of excess IS, under heterogeneous conditions, the initially formed mono-adduct **3g** (Table 3) preferentially undergoes oxidative acylation at the less sterically hindered hydroxymethyl group of the HMF moiety.

At this stage of our study, fabrication of packed-bed mesoreactors **R** was considered to set up an effective flow procedure for the synthesis of *exo*-MAIs **3** promoted by **G** (Table 7). Accordingly, a pressure-resistant stainless steel column (length, 10 cm; internal diameter, 0.46 cm) was filled with **G** by the slurry packing technique (DCM as the swelling solvent). Then, pycnometry measurements were conducted to determine the hold-up (dead) volume (V_o) and the total porosity (ε_{tot}) of reactor **R** and calculate the residence time at different flow rates (Supporting Information).

Table 6. Regioselective Synthesis of *exo*-MAIs 3a−f,h under Heterogeneous Conditions[a]

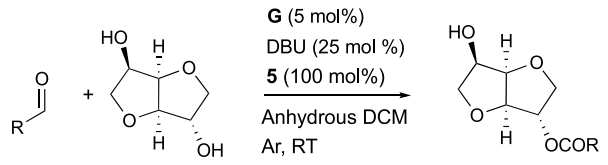

1 2 3

entry	aldehyde 1	*exo*-MAI **3**	yield (%)[b]	exo/endo[c]
1	**1a**	**3a**	75	4.4
2	**1b**	**3b**	72	4.3
3	**1c**	**3c**	73	4.0
4	**1d**	**3d**	69	3.6
5	**1e**	**3e**	77	4.3
6	**1f**	**3f**	78	5.3
7	**1h**	**3h**	79	4.4

[a]**1a−f,h** (0.5 mmol), **2** (1.5 mmol), and anhydrous DCM (4.0 mL). [b]Isolated yield. [c]Selectivity detected by ^{1}H NMR of the crude reaction mixture.

Flow experiments were performed with a two-pump, three-way valve apparatus depicted in Table 8 initially using the model benzoylation for optimization (entry 1). After some experimentation, the reagent concentrations and flow rates were conveniently adjusted to reach the reaction completion and, therefore, facilitate purification of the target MAI **3a**. Hence, reactor **R** was independently fed with continuously degassed (argon) mixtures of IS **2** (0.75 M)/**1a** (0.25 M) and DBU (0.06 M)/**5** (0.25 M) at 0.1 mL min^{-1}. Under these optimized conditions, the steady-state regime was achieved in 45 min, and MAI **3a** was recovered with good regioselectivity (exo/endo = 4.6) without the detection of the undesired diester.

Pleasantly, the process output remained unaltered for ca. 110 h; after that time, however, a progressive loss of conversion efficiency accompanied by a concomitant little increase of regioselectivity was observed (Figure 3). Overall, the long-term stability study with **R** showed a total TON of 146 for heterogeneous **G** and a satisfactory productivity (P) in flow regime (**3a**: 1.32 mmol h^{-1} mmol$_{cat}^{-1}$; entry 1). Similarly, the selected aldehydes **1c,e,f,h** were engaged in the CF esterification of IS furnishing MAIs **3c,e,f,h** with high conversions (>90%) through the controlled variation of residence times (entries 2−5).

As already commented, **IS-5MN** is a commercial vasodilator with a favorable pharmacokinetic profile and also a chiral scaffold of current interest for diversified therapeutic uses.[23,65] As such, several synthetic strategies to **IS-5MN** have been developed by exo-selective IS acylation, exploiting the DCC−DMAP−carboxylic acid system[23] or enzymatic transesterifications with vinyl esters.[35] Due to the growing impact of organocatalysis in the CF manufacturing of APIs,[68,69] we considered the multigram, flow synthesis of **3a** as the key step of a benzoylation/nitration/deprotection sequence leading to **IS-5MN** (Scheme 4). Accordingly, the reactor **R** was operated for 24 h under the conditions of entry 1 (Table 7), providing 3.2 g of **3a** after purification. Then, subsequent nitration (HNO_3 and Ac_2O) and benzoyl group deprotection (KOH) were run in batch, affording pure **IS-5MN** (recrystallization) in 75% yield over two steps.

https://doi.org/10.1021/acssuschemeng.1c02765
ACS Sustainable Chem. Eng. 2021, 9, 8295−8305

Scheme 3. IS Acylation with HMF Using Heterogeneous Triazolium Salt G

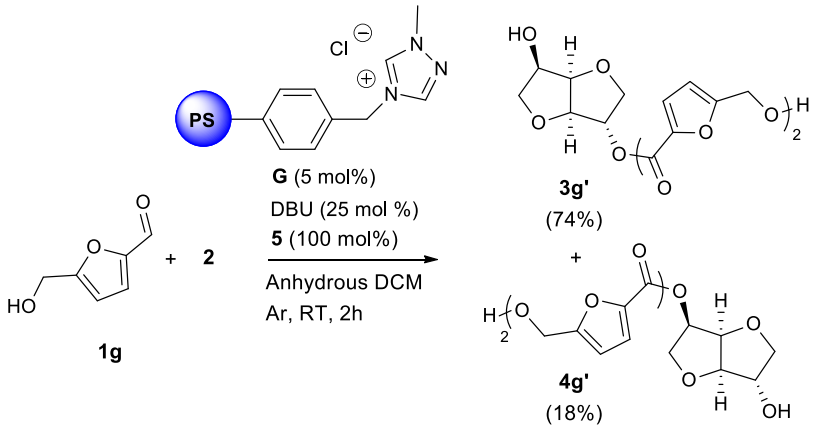

Table 7. Main Features of the Packed-Bed Mesoreactor R

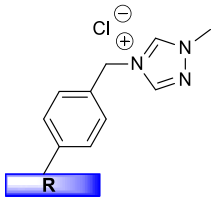

(loaded **G**, *f*: 0.47 mmol g^{-1})

loaded **G** [g][a]	V_G [mL][b]	V_o [mL][c]	total porosity[d]	time [min][e]	pressure [bar][f]
1.2	1.66	1.29	0.78	26	3

[a]Calculated by the difference with the catalyst amount in the residual slurry solution. [b]Geometric volume (V_G) of the stainless steel column. [c]Void volume (V_o) determined by pycnometry. [d]Total porosity $\varepsilon_{tot} = V_o/V_G$. [e]Residence time calculated at 50 μL min^{-1}. [f]Back-pressure measured at 50 μL min^{-1} (RT, DCM).

Table 8. CF Production of *exo*-MAIs 3[a]

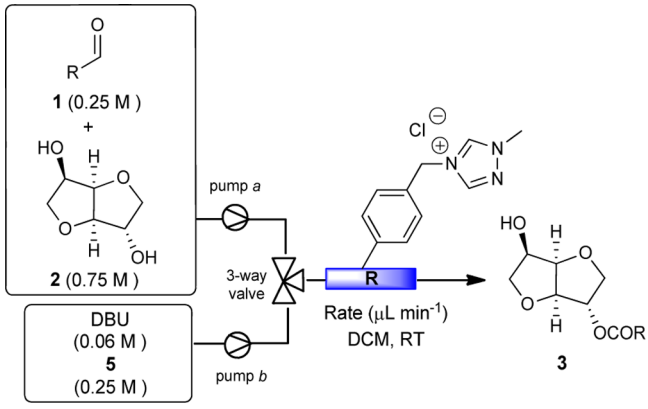

entry	*exo*-MAI **3** (conv. [%])[b]	rate (μL min^{-1})	exo/endo[c]	P^d
1	**3a** (>95)	100	4.6	1.32
2	**3c** (>95)	100	4.0	1.32
3	**3e** (90)	40	4.3	0.48
4	**3f** (>95)	100	5.3	1.32
5	**3h** (93)	100	4.3	1.24

[a]See the Supporting Information for a description of the flow apparatus. [b]Instant conversion in the steady-state regime, as determined by ^{1}H NMR analysis. [c]Established by ^{1}H NMR analysis of the collected reaction mixture. [d]Productivities (P) are measured in mmol h^{-1} $mmol_{cat}^{-1}$ (see the Supporting Information for details).

CONCLUSIONS

In summary, we have presented a novel strategy for the regiodivergent monoesterification of IS based on oxidative NHC catalysis. Good levels of endo- and exo-selectivities were achieved with representative classes of aldehydes that served as mild acylating agents, including the bio-based HMF. Process intensification was addressed by the immobilization on the polystyrene support of the active triazolium salt precatalyst and fabrication of the corresponding fixed-bed mesoreactor for moving from batch to CF conditions. Elucidation of the actual role of azolium salt stereoelectronics and solvent effect in directing endo- or exo-selectivity is currently underway by a detailed density functional theory study that will be reported in due course.

EXPERIMENTAL SECTION

Reagents, solvents, and the CF apparatus used in this study are listed and described in the Supporting Information.

General Procedure for the Regioselective Synthesis of *exo*-MAIs 3a–h under Homogeneous Conditions. A stirred mixture of aldehyde **1** (0.5 mmol), IS **2** (1.5 or 10 mmol for **3g** synthesis), oxidant **5** (204 mg, 0.5 mmol), and precatalyst **C** (6 mg, 0.025 mmol) in anhydrous THF (4 mL) was degassed under vacuum and saturated with argon (by an Ar-filled balloon) three times. Then, DBU was added (18 μL, 0.12 mmol), and the reaction mixture was stirred at room temperature until almost complete aldehyde consumption was detected [thin-layer chromatography (TLC) analysis]. After the solvent removal, EtOAc (15 mL) was added, and the resulting organic solution was washed with water (3 × 5 mL). The organic layer was dried (Na_2SO_4), concentrated, and eluted from a column of silica gel with a suitable elution system to give, in order of elution, diester **6**, *exo*-MAI **3**, and *endo*-MAI **4**.

General Procedure for the Regioselective Synthesis of *endo*-MAIs 4a–h under Homogeneous Conditions. A stirred mixture of aldehyde **1** (0.5 mmol), IS **2** (1.5 or 10 mmol for **4g** synthesis), oxidant **5** (204 mg, 0.5 mmol), and precatalyst **D** (10 mg, 0.025 mmol) in anhydrous DMSO (4 mL) was degassed under vacuum and saturated with argon (by an Ar-filled balloon) three times. Then, NEt_3 was added (16 μL, 0.12 mmol), and the reaction mixture was stirred at room temperature until almost complete aldehyde consumption was detected (TLC analysis). After the solvent removal (freeze-drying), EtOAc (15 mL) was added, and the resulting organic solution was washed with water (3 × 5 mL). The organic layer was dried (Na_2SO_4), concentrated, and eluted from a column of silica gel with a suitable elution system to give, in order of elution, diester **6**, *exo*-MAI **3**, and *endo*-MAI **4**.

CF Synthesis of *exo*-MAIs 3. The mesoreactor **R** was independently fed with continuously degassed mixtures of IS **2** (0.75

https://doi.org/10.1021/acssuschemeng.1c02765
ACS Sustainable Chem. Eng. 2021, 9, 8295–8305

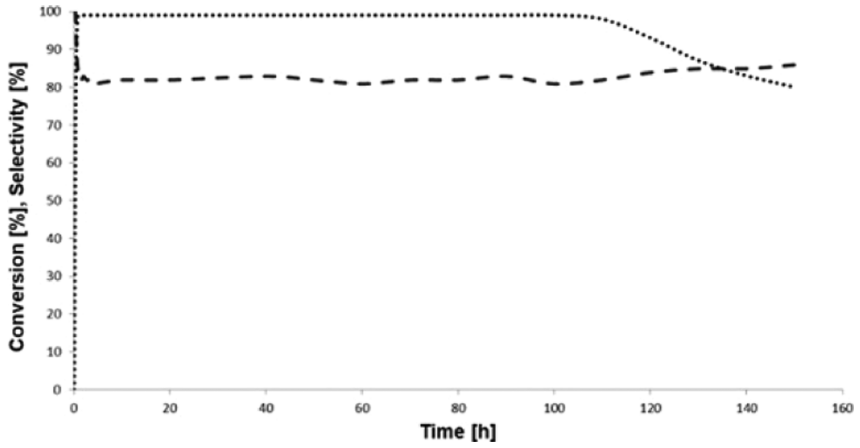

Figure 3. Long-term stability experiment (**1a**–IS coupling). Conversion [%], dotted line; **3a** selectivity [%], dashed line.

Scheme 4. Three-Step (Flow and Batch) Synthesis of IS-5MN

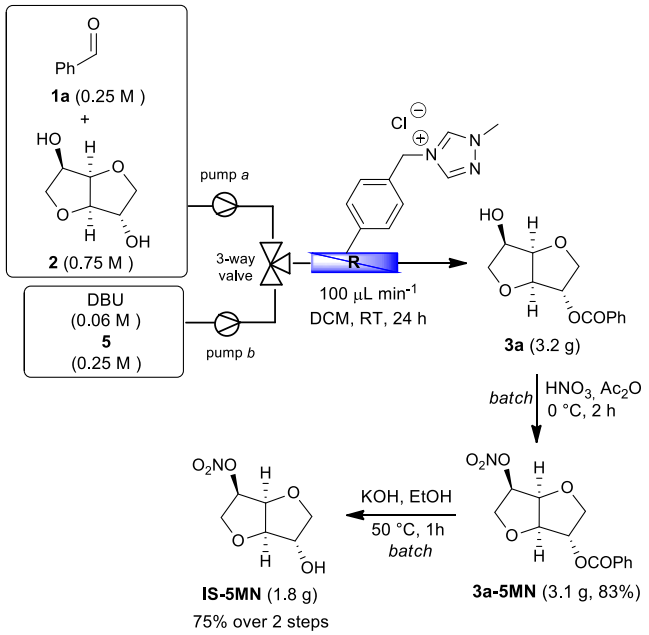

M)/**1** (0.25 M) delivered by channel A and DBU (0.06 M)/**5** (0.25 M) delivered by channel B. Flow rates ranged from 40 to 100 μL min^{-1}, allowing high levels of substrate conversion (≥90%). The mesoreactor **R** was operated for 5 h under steady-state conditions. After this period, the collected reaction mixture was concentrated, dissolved in EtOAc (100 mL), and washed with water (3 × 30 mL). The organic layer was dried (Na_2SO_4), concentrated, and eluted from a column of silica gel with a suitable elution system to give first the alcohol **5′** and then, in order of elution, *exo*-MAI **3** and *endo*-MAI **4**.

■ ASSOCIATED CONTENT

Supporting Information

The Supporting Information is available free of charge at https://pubs.acs.org/doi/10.1021/acssuschemeng.1c02765.

General experimental procedures; reaction scope under heterogeneous conditions; multistep synthesis of **IS-5MN**; and ^{1}H NMR, and ^{13}C NMR spectra of **3**, **4**, and **6** (PDF)

■ AUTHOR INFORMATION

Corresponding Authors

Daniele Ragno − *Department of Chemical, Pharmaceutical and Agricultural Sciences, University of Ferrara, 44121 Ferrara, Italy;* orcid.org/0000-0003-0016-290X; Email: daniele.ragno@unife.it

Alessandro Massi − *Department of Chemical, Pharmaceutical and Agricultural Sciences, University of Ferrara, 44121 Ferrara, Italy;* orcid.org/0000-0001-8303-5441; Email: alessandro.massi@unife.it

Authors

Costanza Leonardi − *Department of Chemical, Pharmaceutical and Agricultural Sciences, University of Ferrara, 44121 Ferrara, Italy*

Graziano Di Carmine − *Department of Chemical, Pharmaceutical and Agricultural Sciences, University of Ferrara, 44121 Ferrara, Italy*

Olga Bortolini − *Department of Chemical, Pharmaceutical and Agricultural Sciences, University of Ferrara, 44121 Ferrara, Italy;* orcid.org/0000-0002-8428-2310

Arianna Brandolese − *Department of Chemical, Pharmaceutical and Agricultural Sciences, University of Ferrara, 44121 Ferrara, Italy*

Carmela De Risi − *Department of Chemical, Pharmaceutical and Agricultural Sciences, University of Ferrara, 44121 Ferrara, Italy;* orcid.org/0000-0001-8162-6782

Complete contact information is available at: https://pubs.acs.org/10.1021/acssuschemeng.1c02765

Author Contributions

The manuscript was written through contributions of all authors. All authors have given approval to the final version of the manuscript.

Notes

The authors declare no competing financial interest.

■ ACKNOWLEDGMENTS

We gratefully acknowledge the University of Ferrara (fondi FAR) for financial support. Thanks are also given to Paolo Formaglio for NMR experiments, to Tatiana Bernardi for HRMS analyses, and to Ercolina Bianchini for elemental analyses.

REFERENCES

(1) Rinaldi, R.; Schüth, F. Design of solid catalysts for the conversion of biomass. *Energy Environ. Sci.* **2009**, *2*, 610−626.

(2) Delbecq, F.; Khodadadi, M. R.; Rodriguez Padron, D.; Varma, R.; Len, C. Isosorbide: Recent advances in catalytic production. *Mol. Catal.* **2020**, *482*, 110648.

(3) Bonnin, I.; Mereau, R.; Tassaing, T.; De Oliveira Vigier, K. One-pot synthesis of isosorbide from cellulose or lignocellulosic biomass: a challenge? *Beilstein J. Org. Chem.* **2020**, *16*, 1713−1721.

(4) Rose, M.; Palkovits, R. Isosorbide as a Renewable Platform chemical for Versatile Applications-Quo Vadis? *ChemSusChem* **2012**, *5*, 167−176.

(5) Dussenne, C.; Delaunay, T.; Wiatz, V.; Wyart, H.; Suisse, I.; Sauthier, M. Synthesis of isosorbide: an overview of challenging reactions. *Green Chem.* **2017**, *19*, 5332−5344.

(6) Abshagen, U.; Spoer-Radun, S. First data on effects and pharmacokinetics of isosorbide-5-mononitrate in normal man. *Eur. J. Clin. Pharmacol.* **1981**, *19*, 423−429.

(7) Zhu, S.-G.; Yang, J.-T.; Zhang, G.-M.; Chen, C.-F.; Zhang, F.-L. An Improved Process for Industrial Production of Isosorbide-5-mononitrate: Recycling of Wastes. *Org. Process Res. Dev.* **2018**, *22*, 991−995.

(8) Lavergne, A.; Moity, L.; Molinier, V.; Aubry, J.-M. Volatile short-chain amphiphiles derived from isosorbide: Hydrotropic properties of esters vs. ethers. *RSC Adv.* **2013**, *3*, 5997−6007.

(9) Reddy, T. V. K.; Rani, G. S.; Prasad, R. B. N.; Devi, B. L. A. P. Green recyclable SO_3H-carbon catalyst for the selective synthesis of isomannide-based fatty acid monoesters as non-ionic bio-surfactants. *RSC Adv.* **2015**, *5*, 40997−41005.

(10) Stoer, C.; Nieendick, C.; Weissenegger, M.; Prinz, D.; Winzek, M.; Schoss, J.; Dierker, M.; Boyxen, N.; Griesbach, U.; Seipel, W.; Mauer, W. A use of isosorbide monooleate. WO 2016008747 A1, 2015.

(11) Cui, C.; Zhen, Y.; Qu, J.; Chen, B.; Tan, T. Synthesis of biosafe isosorbide dicaprylate ester plasticizer by lipase in a solvent-free system and its sub-chronic toxicity in mice. *RSC Adv.* **2016**, *6*, 11959−11966.

(12) Yin, B.; Hakkarainen, M. Oligomeric isosorbide esters as alternative renewable resource plasticizers for PVC. *J. Appl. Polym. Sci.* **2011**, *119*, 2400−2407.

(13) Storbeck, R.; Rehahn, M.; Ballauff, M. Synthesis and properties of high-molecular-weight polyesters based on 1,4:3,6-dianhydrohexitols and terephthalic acid. *Makromol. Chem.* **1993**, *194*, 53−64.

(14) Storbeck, R.; Ballauff, M. Synthesis and thermal analysis of copolyesters deriving from 1,4:3,6-dianhydrosorbitol, ethylene glycol, and terephthalic acid. *J. Appl. Polym. Sci.* **1996**, *59*, 1199−1202.

(15) Gandini, A.; Coelho, D.; Gomes, M.; Reis, B.; Silvestre, A. Materials from renewable resources based on furan monomers and furan chemistry: work in progress. *J. Mater. Chem.* **2009**, *19*, 8656−8664.

(16) Wu, J.; Eduard, P.; Jasinska-Walc, L.; Rozanski, A.; Noordover, B. A. J.; van Es, D. S.; Koning, C. E. Fully Isohexide-Based Polyesters: Synthesis, Characterization, and Structure−Properties Relations. *Macromolecules* **2013**, *46*, 384−394.

(17) Sadler, J. M.; Nguyen, A.-P. T.; Toulan, F. R.; Szabo, J. P.; Palmese, G. R.; Scheck, C.; Lutgen, S.; La Scala, J. J. Isosorbide-methacrylate as a bio-based low viscosity resin for high performance thermosetting applications. *J. Mater. Chem. A* **2013**, *1*, 12579−12586.

(18) Al-Naji, M.; Schlaad, H.; Antonietti, M. New (and Old) Monomers from Biorefineries to Make Polymer Chemistry More Sustainable. *Macromol. Rapid Commun.* **2020**, *42*, 2000485.

(19) Chen, J.; Wu, J.; Qi, J.; Wang, H. Systematic Study of Thermal and (Bio)Degradable Properties of Semiaromatic Copolyesters Based on Naturally Occurring Isosorbide. *ACS Sustainable Chem. Eng.* **2019**, *7*, 1061−1071.

(20) Chebbi, Y.; Kasmi, N.; Majdoub, M.; Cerruti, P.; Scarinzi, G.; Malinconico, M.; Dal Poggetto, G.; Papageorgiou, G. Z.; Bikiaris, D. N. Synthesis, Characterization, and Biodegradability of Novel Fully Biobased Poly(decamethylene-co-isosorbide 2,5-furandicarboxylate) Copolyesters with Enhanced Mechanical Properties. *ACS Sustainable Chem. Eng.* **2019**, *7*, 5501−5514.

(21) Meninno, S. Valorization of Waste: Sustainable Organocatalysts from Renewable Resources. *ChemSusChem* **2020**, *13*, 439−468.

(22) Jopp, S. Carbohydrate Based Ionic Liquids (CHILs): Synthesis and Applications. *Eur. J. Org. Chem.* **2020**, *2020*, 6418−6428.

(23) Gilmer, J. F.; Moriarty, L. M.; McCafferty, D. F.; Clancy, J. M. Synthesis, hydrolysis kinetics and anti-platelet effects of isosorbide mononitrate derivatives of aspirin. *Eur. J. Pharm. Sci.* **2001**, *14*, 221−227.

(24) Matt, L.; Parve, J.; Parve, O.; Pehk, T.; Pham, T. H.; Liblikas, I.; Vares, L.; Jannasch, P. Enzymatic Synthesis and Polymerization of Isosorbide-Based Monomethacrylates for High-T_g Plastics. *ACS Sustainable Chem. Eng.* **2018**, *6*, 17382−17390.

(25) Laanesoo, S.; Bonjour, O.; Parve, J.; Parve, O.; Matt, L.; Vares, L.; Jannasch, P. Poly(alkanoyl isosorbide methacrylate)s: From Amorphous to Semicrystalline and Liquid Crystalline Biobased Materials. *Biomacromolecules* **2021**, *22*, 640−648.

(26) Stoss, P.; Merrath, P.; Schlüter, G. Regioselective Acylation of 1,4:3,6-Dianhydro-D-glucitol. *Synthesis* **1987**, *1987*, 174−176.

(27) Berini, C.; Lavergne, A.; Molinier, V.; Capet, F.; Deniau, E.; Aubry, J.-M. Iodoetherification of Isosorbide-Derived Glycals: Access to a Variety of O-Alkyl or O-Aryl Isosorbide Derivatives. *Eur. J. Org. Chem.* **2013**, *2013*, 1937−1949.

(28) Abenhaïm, D.; Loupy, A.; Munnier, L.; Tamion, R.; Marsais, F.; Quéguiner, G. Selective alkylations of 1,4: 3,6-dianhydro-D-glucitol (isosorbide). *Carbohydr. Res.* **1994**, *261*, 255−266.

(29) Gallagher, J. J.; Hillmyer, M. A.; Reineke, T. M. Isosorbide-based Polymethacrylates. *ACS Sustainable Chem. Eng.* **2015**, *3*, 662−667.

(30) Shaikh, A. L.; Kale, A. S.; Shaikh, M. A.; Puranik, V. G.; Deshmukh, A. R. A. S. Asymmetric synthesis of β-lactams by [2+2] cycloaddition using 1,4:3,6-dianhydro-D-glucitol (isosorbide) derived chiral pools. *Tetrahedron* **2007**, *63*, 3380−3388.

(31) Čeković, Ž.; Tokić, Z. Selective esterification of 1, 4: 3, 6-dianhydro-D-glucitol. *Synthesis* **1989**, *1989*, 610−612.

(32) Mukesh, D.; Sheth, D.; Mokashi, A.; Wagh, J.; Tilak, J. M.; Banerji, A. A.; Thakkar, K. R. Lipase catalysed esterification of isosorbide and sorbitol. *Biotechnol. Lett.* **1993**, *15*, 1243−1246.

(33) Seemayer, R.; Bar, N.; Schneider, M. P. Enzymatic preparation of isomerically pure 1,4:3,6-dianhydro-D-glucitol monoacetates - precursors for isoglucitol 2- and 5-mononitrates. *Tetrahedron: Asymmetry* **1992**, *3*, 1123−1126.

(34) Zhu, S.-G.; Huang, J.-X.; Zhang, G.-M.; Chen, S.-X.; Zhang, F.-L. Development of a Practical Enzymatic Synthesis of Isosorbide-2-acetate. *Org. Process Res. Dev.* **2018**, *22*, 1548−1552.

(35) Brown, C.; Marston, R. W.; Quigley, P. F.; Roberts, S. M. New preparative routes to isosorbide 5-mononitrate. *J. Chem. Soc., Perkin Trans. 1* **2000**, 1809−1810.

(36) Kielty, P.; Smith, D. A.; Cannon, P.; Carty, M. P.; Kennedy, M.; McArdle, P.; Singer, R. J.; Aldabbagh, F. Selective Methylmagnesium Chloride Mediated Acetylations of Isosorbide: A Route to Powerful Nitric Oxide Donor Furoxans. *Org. Lett.* **2018**, *20*, 3025−3029.

(37) Ragno, D.; Brandolese, A.; Di Carmine, G.; Buoso, S.; Belletti, G.; Leonardi, C.; Bortolini, O.; Bertoldo, M.; Massi, A. Exploring Oxidative NHC-Catalysis as Organocatalytic Polymerization Strategy towards Polyamide Oligomers. *Chem.—Eur. J.* **2021**, *27*, 1839−1848.

(38) Ragno, D.; Di Carmine, G.; Brandolese, A.; Bortolini, O.; Giovannini, P. P.; Fantin, G.; Bertoldo, M.; Massi, A. Oxidative NHC-Catalysis as Organocatalytic Platform for the Synthesis of Polyester Oligomers by Step-Growth Polymerization. *Chem.—Eur. J.* **2019**, *25*, 14701−14710.

(39) Ragno, D.; Brandolese, A.; Urbani, D.; Di Carmine, G.; De Risi, C.; Bortolini, O.; Giovannini, P. P.; Massi, A. Esterification of glycerol and solketal by oxidative NHC-catalysis under heterogeneous batch and flow conditions. *React. Chem. Eng.* **2018**, *3*, 816−825.

(40) Brandolese, A.; Ragno, D.; Di Carmine, G.; Bernardi, T.; Bortolini, O.; Giovannini, P. P.; Pandoli, O. G.; Altomare, A.; Massi, A. Aerobic oxidation of 5-hydroxymethylfurfural to 5-hydroxymethyl-2-furancarboxylic acid and its derivatives by heterogeneous NHC-catalysis. *Org. Biomol. Chem.* **2018**, *16*, 8955−8964.

https://doi.org/10.1021/acssuschemeng.1c02765
ACS Sustainable Chem. Eng. 2021, 9, 8295−8305

(41) Wang, M. H.; Scheidt, K. A. Cooperative Catalysis and Activation with N-Heterocyclic Carbenes. *Angew. Chem., Int. Ed.* **2016**, *55*, 14912−14922.
(42) Mahatthananchai, J.; Bode, J. W. On the Mechanism of N-Heterocyclic Carbene-Catalyzed Reactions Involving Acyl Azoliums. *Acc. Chem. Res.* **2014**, *47*, 696−707.
(43) De Sarkar, S.; Biswas, A.; Samanta, R. C.; Studer, A. Catalysis with N-Heterocyclic Carbenes under Oxidative Conditions. *Chem.—Eur. J.* **2013**, *19*, 4664−4678.
(44) Knappke, C. E. I.; Imami, A.; von Wangelin, A. J. Oxidative N-Heterocyclic Carbene Catalysis. *ChemCatChem* **2012**, *4*, 937−941.
(45) The bulky structure of acyl azolium salts generated in the presence of the quinone oxidant **5** has been proposed in an our previous study on the basis of DFT calculations: Di Carmine, G.; Ragno, D.; Brandolese, A.; Bortolini, O.; Pecorari, D.; Sabuzi, F.; Mazzanti, A.; Massi, A. Enantioselective Desymmetrization of 1,4-Dihydropyridines by Oxidative NHC Catalysis. *Chem.—Eur. J.* **2019**, *25*, 7469−7474.
(46) For a detailed study on the intermolecular hydrogen bonding between metal chlorides and isosorbide and its effect on regioselectivity, see: Zhang, M.; Lai, W.; Su, L.; Lin, Y.; Wu, G. A synthetic strategy toward isosorbide polycarbonate with a high molecular weight: the effect of intermolecular hydrogen bonding between isosorbide and metal chlorides. *Polym. Chem.* **2019**, *10*, 3380−3389.
(47) Myles, L.; Gathergood, N.; Connon, S. J. The catalytic versatility of low toxicity dialkyltriazolium salts: in situ modification facilitates diametrically opposed catalysis modes in one pot. *Chem. Commun.* **2013**, *49*, 5316−5318.
(48) Grabowski, S. J. Hydrogen Bonds with BF_4^- Anion as a Proton Acceptor. *Crystals* **2020**, *10*, 460.
(49) Yuan, B.; He, R.; Guo, X.; Shen, W.; Zhang, F.; Xu, Y.; Li, M. DFT study on the Au(I)-catalyzed cyclization of indole-allenoate: Effects of counterion and solvent. *New J. Chem.* **2018**, *42*, 15618−15628.
(50) Di Carmine, G.; Abbott, A. P.; D'Agostino, C. Deep eutectic solvents: alternative reaction media for organic oxidation reactions. *React. Chem. Eng.* **2021**, *6*, 582−598.
(51) Gandeepan, P.; Kaplaneris, N.; Santoro, S.; Vaccaro, L.; Ackermann, L. Biomass-Derived Solvents for Sustainable Transition Metal-Catalyzed C-H Activation. *ACS Sustainable Chem. Eng.* **2019**, *7*, 8023−8040.
(52) Clarke, C. J.; Tu, W.-C.; Levers, O.; Bröhl, A.; Hallett, J. P. Green and Sustainable Solvents in Chemical Processes. *Chem. Rev.* **2018**, *118*, 747−800.
(53) Alder, C. M.; Hayler, J. D.; Henderson, R. K.; Redman, A. M.; Shukla, L.; Shuster, L. E.; Sneddon, H. F. Updating and further expanding GSK's solvent sustainability guide. *Green Chem.* **2016**, *18*, 3879−3890.
(54) Gu, Y.; Jérôme, F. Bio-based solvents: an emerging generation of fluids for the design of eco-efficient processes in catalysis and organic chemistry. *Chem. Soc. Rev.* **2013**, *42*, 9550−9570.
(55) Zhang, Q.; De Oliveira Vigier, K.; Royer, S.; Jérôme, F. Deep eutectic solvents: syntheses, properties and applications. *Chem. Soc. Rev.* **2012**, *41*, 7108−7146.
(56) Abbott, A. P.; Capper, G.; Davies, D. L.; Rasheed, R. K.; Tambyrajah, V. Novel solvent properties of choline chloride/urea mixtures. *Chem. Commun.* **2003**, 70−71.
(57) Prat, D.; Pardigon, O.; Flemming, H.-W.; Letestu, S.; Ducandas, V.; Isnard, P.; Guntrum, E.; Senac, T.; Ruisseau, S.; Cruciani, P.; Hosek, P. Sanofi's Solvent Selection Guide: A Step Toward More Sustainable Processes. *Org. Process Res. Dev.* **2013**, *17*, 1517−1525.
(58) Henderson, R. K.; Jiménez-González, C.; Constable, D. J. C.; Alston, S. R.; Inglis, G. G. A.; Fisher, G.; Sherwood, J.; Binks, S. P.; Curzons, A. D. Expanding GSK's solvent selection guide—embedding sustainability into solvent selection starting at medicinal chemistry. *Green Chem.* **2011**, *13*, 854−862.
(59) Cseri, L.; Razali, M.; Pogany, P.; Szekely, G. Organic Solvents in Sustainable Synthesis and Engineering. In *Green Chemistry: An Inclusive Approach*; Török, B., Dransfield, T., Eds.; Elsevier: Amsterdam, 2018; Chapter 3.15, pp 513−553.
(60) Zang, H.; Wang, K.; Zhang, M.; Xie, R.; Wang, L.; Chen, E. Y.-X. Catalytic coupling of biomass-derived aldehydes into intermediates for biofuels and materials. *Catal. Sci. Technol.* **2018**, *8*, 1777−1798.
(61) Gupta, N. K.; Fukuoka, A.; Nakajima, K. Metal-Free and Selective Oxidation of Furfural to Furoic Acid with an N-Heterocyclic Carbene Catalyst. *ACS Sustainable Chem. Eng.* **2018**, *6*, 3434−3442.
(62) De Risi, C.; Bortolini, O.; Brandolese, A.; Di Carmine, G.; Ragno, D.; Massi, A. Recent advances in continuous-flow organocatalysis for process intensification. *React. Chem. Eng.* **2020**, *5*, 1017−1052.
(63) Ragno, D.; Di Carmine, G.; Brandolese, A.; Bortolini, O.; Giovannini, P. P.; Massi, A. Immobilization of Privileged Triazolium Carbene Catalyst for Batch and Flow Stereoselective Umpolung Processes. *ACS Catal.* **2017**, *7*, 6365−6375.
(64) Bortolini, O.; Cavazzini, A.; Dambruoso, P.; Giovannini, P. P.; Caciolli, L.; Massi, A.; Pacifico, S.; Ragno, D. Thiazolium-functionalized polystyrene monolithic microreactors for continuous-flow umpolung catalysis. *Green Chem.* **2013**, *15*, 2981−2992.
(65) Santschi, N.; Wagner, S.; Daniliuc, C.; Hermann, S.; Schäfers, M.; Gilmour, R. Synthesis of 2-[^{18}F]Fluoro-2-deoxyisosorbide 5-mononitrate and Assessment of Its in vivo Biodistribution as Determined by Dynamic Positron Emission Tomography (PET). *ChemMedChem* **2015**, *10*, 1724−1732.
(66) Borah, P.; Fianchini, M.; Pericàs, M. A. Assessing the Role of Site Isolation and Compartmentalization in Packed-Bed Flow Reactors for Processes Involving Wolf-and-Lamb Scenarios. *ACS Catal.* **2021**, *11*, 6234−6242.
(67) van den Berg, H. J.; Challa, G.; Pandit, U. K. Polymer-bound thiamine models. III. Influence of site isolation on the catalytic activity of polystyrene-bound thiazolium salts. *React. Polym.* **1989**, *11*, 101−116.
(68) Porta, R.; Benaglia, M.; Puglisi, A. Flow Chemistry: Recent Developments in the Synthesis of Pharmaceutical Products. *Org. Process Res. Dev.* **2016**, *20*, 2−25.
(69) Atodiresei, I.; Vila, C.; Rueping, M. Asymmetric Organocatalysis in Continuous Flow: Opportunities for Impacting Industrial Catalysis. *ACS Catal.* **2015**, *5*, 1972−1985.

https://doi.org/10.1021/acssuschemeng.1c02765
ACS Sustainable Chem. Eng. 2021, 9, 8295−8305